Journal of Renewable Materials
DOI:10.32604/jrm.2020.09304
Article

Tech Science Press

Preparation and Characterization of Tung Oil Toughened Modified Phenolic Foams with Enhanced Mechanical Properties and Smoke Suppression

Fei Song[1,2], Puyou Jia[1,*], Caiying Bo[1], Xiaoli Ren[1], Lihong Hu[1] and Yonghong Zhou[1,*]

[1]Institute of Chemical Industry of Forest Products, Chinese Academy of Forestry, National Engineering Laboratory for Biomass Chemical Utilization, Co-Innovation Center of Efficient Processing and Utilization of Forest Resources, Key Laboratory of Chemical Engineering of Forest Products, National Forestry and Grassland Administration, Key Laboratory of Biomass Energy and Materials, Nanjing, 210042, China
[2]Nanjing Forestry University, Nanjing, 210037, China
*Corresponding Authors: Puyou Jia. Email: jiapuyou@icifp.cn; Yonghong Zhou. Email: yhzhou777@sina.com
Received: 01 December 2019; Accepted: 20 January 2020

Abstract: In this study, we prepared a series of tung oil phenolic foams (TPF) by a one-pot method. The FT-IR and ^{1}H NMR spectra confirm the successful Friedel-Crafts grafting of phenol to the long-chain alkyl group in tung oil. Modified TPFs exhibit enhanced mechanical properties, including compressive and flexural strengths of up to 0.278 ± 0.036 MPa and 0.450 ± 0.017 MPa, respectively, which represent increases of 68.75% and 86.72% over those of pure phenolic foam (PF). SEM spectra reveal the TPF microstructure to have uniform hexagonal cell morphology, narrower cell size distribution, and smaller mean cell size, suggesting enhanced mechanical properties. The TPF total smoke release decreased by 74.23%, indicating that the long alkyl chain significantly improves smoke suppression of the combusting foam. However, due to the flammability of the alkyl chains, the TPF limiting oxygen index decreases with increasing tung oil content. Moreover, TPF exhibits reduced thermal stability and high-temperature charring rate, elevated peak and mean heat release rates, and higher total heat release compared with pure PF. Therefore, future research will focus on the use of tung oil modified flame retardant to provide more robust phenolic foams.

Keywords: Tung oil; Friedel-Craft reaction; phenolic foams; mechanical properties; smoke suppression

1 Introduction

Phenolic foams (PFs) possess excellent fire resistance; they have application as flame retardants, heat insulation materials, and they provide flame penetration resistance with low smoke and low toxicity during combustion [1,2]. There is an increasing demand for heat insulation and fire protection materials as well as the traditional insulation materials (such as polystyrene [3,4] and polyurethane foams [5]) exist serious shortcomings that is flammability and produce a large amount of highly toxic fumes and drips during combustion process [6]. PFs have seen rapid development in recent years and are among the fastest-growing categories of foam. Also, the PF molecular structure contains a benzene ring connected via an easily oxidizable methylene linkage. This feature reduces toughness and makes PF materials

susceptible to pulverization, severely limiting its opportunities for post-manufacture processing and application [7,8]. Therefore, it is crucial to research methods to reduce brittleness and improve the robustness of PF materials.

During recent decades, researchers have developed a variety of different methods to toughen PFs [9,10]. These approaches broadly fall into two categories: physical blending and chemical modification [11]. Chemical modification can provide a remarkable toughening effect by introducing long flexible chains into the rigid phenol-resin skeleton, a technique that has attracted much research interest [12,13]. Most toughening agents derive from limited petrochemical reserves, and their continued use is a significant drain on resources. Biomass resources are abundant, inexpensive, and renewable. Therefore, the use of renewable biomass to replace petroleum-sourced products is gaining popularity. Biomass chemicals have applications in toughening phenolic foams, including lignin [14,15], cardanol [16,17], tannin [18], and cellulose [19].

Tung oil is an industrial vegetable oil extracted from the seeds of the tung tree. This lustrous oil is the highest quality drying in vegetable oil available [13,20]. The main component of tung oil is octadeca-9,11,13-trienoic acid glyceride, which accounts for 73%–80% of the tung oil composition [21]. China has the best quality tung oil available, and produces more than 100 thousand tons per annum, which is close to 80% of the total worldwide production [22]. The molecular structure of tung oil features a unique conjugated triene bond that is not present in other vegetable oils. Therefore, tung oil is chemically reactive and multiple reactions, including Friedel-Crafts, Diels-Alder, epoxidation, aminolysis, alcoholysis, and radical polymerization reactions [23]. Researchers have developed a range of products, including polyester [24], polyurethane [5], UV-curable resin [25,26], and plasticizer [27,28], using tung oil as the raw material. Literature reports of the modification of by using the Friedel-Crafts reaction reveal that after curing, the tung oil modified phenolic resin is more robust and exhibits improved wear resistance [29,30]. These properties may suit application as a high-temperature friction material such as brake pad linings [31,32]. However, these reports focus on phenolic plastics produced by linear polycondensation. We were unable to find any literature reports of tung oil toughened PF materials provided by three dimensional polycondensation. Thus, we propose to prepare resol-phenolic resin by a one-pot method using the Friedel-Crafts reaction to combine tung oil with phenol. We will then process the resin to obtain the tung oil toughened phenolic foam (Fig. 1). We characterized the properties of PF foam samples, including their mechanical properties, microstructure, thermal stability, limiting oxygen index (LOI), flame retardancy and smoke suppression.

2 Experimental Section

2.1 Materials

Tung oil (TO) was purchased from the Nanjing Daziran Fine chemicals Co. Ltd (≥ 95%). Phenol, polyformaldehyde, n-pentane, tetrafluoroboric acid (40 wt% in water), Tween 80, NaOH, H_2SO_4, and H_3PO_4 were provided by Shanghai Titan Scientific Co., Ltd. All raw materials were analytical pure and used as received.

2.2 Synthesis of Tung Oil-Toughened Phenolic Foams (TPFs)

First, phenol, TO (in ratio of 3, 6, 9 and 12 wt% to phenol) and 1 wt% tetrafluoroboric acid (40 wt% in water) were added to 500 mL of the four-necked flask provided with a thermocouple, mechanical stirrer, and condenser. The mixture was stirred at 90°C for 1 h and then cooled to 70°C. Second, paraformaldehyde was multiple poured into the reaction system due to a large amount of heat was released when the paraformaldehyde was decomposed, during which the pH was controlled to around 9 by adding an aqueous sodium hydroxide solution (30 wt%). Then, the system was kept heating at 70°C for 2 h and heated to 90°C for 1 h. The pure PF was prepared starting from the second step without Friedel-Crafts

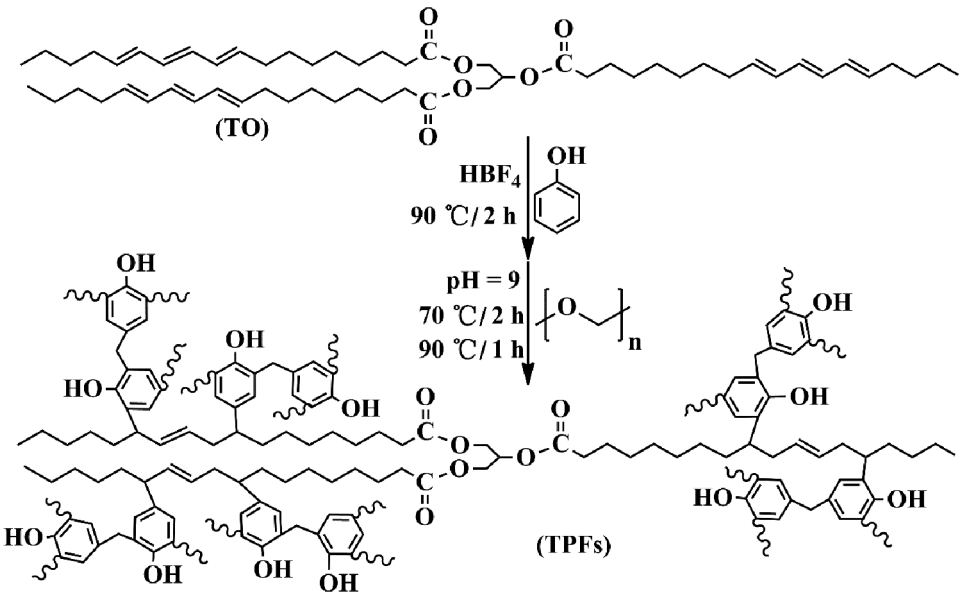

Figure 1: The design and synthetic scheme for TPFs

reaction. The molar ratio of formaldehyde to phenol in all reaction systems was 1.7:1. Third, the phenolic resin prepared above (100 g), Tween 80 (5–6 g), n-pentane (8–10 g) were mixed for 30 s under rapid stirring at 2,000 rpm. The mixed acid curing agent (20 g, water/H_2SO_4/H_3PO_4 = 1/1/1, w/w) was added rapid stirring at 2,000 rpm for 30 s. Finally, the mixture was quickly poured into a stainless steel mold (200 mm × 200 mm × 50 mm) under 80°C for 1 h. Identifications of toughened samples were marked according to the different content of TO. For instance, TPF-5 refer to the foam containing 5 wt % TO.

2.3 Characterizations

FT-IR spectra were recorded by using a Nicolet IS 10 FT-IR spectrometer (Nicolet Co., USA) in a range of 4000-500 cm^{-1} and the resolution of 4 cm^{-1}. ^1H NMR spectra were performed on a Bruker ARX 300 NMR spectrometer with $CDCl_3$ as solvents and tetramethylsilane as the internal standard. Elemental analysis was investigated on a Perkin-Elmer 2400 II elemental Analyzer (USA). The molecular weight of tung oil and pure tung oil-phenol reaction products were carried out using a Gel Permeation Chromatography (GPC) measurement (Waters, USA) at 30°C (fow rate: 1 mL/min, column: mixed PL gel 300 × 718 mm, 25 μm) using HPLC-grade THF as solvent. Tung oil and pure tung oil-phenol reaction products were dissolve in THF solution with concentration of 1 mg/3 mL. Thermogravimetric analysis (TGA) were recorded by a NETZSCH TG 209F1 (Netzsch Instrument Crop., Germany) from 35 to 800°C with a heating rate of 20 °C/min under a oxygen atmosphere. The scanning electron microscopy (SEM, JSM-7600F) was used to observe the morphology of foam with an accelerating voltage of 15 kV after gold sputtering. The software Nano Measurer 1.2 was used to determine mean pore diameter and pore size distribution.

Mechanical properties of the foams were tested on a CMT4000 universal testing machine (Shenzhen Sansi Test Equipment Co., Ltd., China). Each specimen used for the flexural strength test was 120 mm × 25 mm × 20 mm (according to GB/T8812.1-2007) and the compressive strength test was 50 mm × 50 mm × 50 mm (according to GB/T 8813-2008). In both measurements, each sample need test at least three times. The density was determined according to the weight of the foam and the dimensions.

The cone calorimeter tests were performed according to ISO 5660-1:2015 standard on a FTT0007 (NLFRM-05) double analysis cabinet cone calorimeter (UK, FTT). Each sample was 100 mm × 100 mm × 20 mm in size, and bottom and edges wrapped in aluminum foil.

Limiting oxygen index (LOI) was conducted according to GB/T 2406-1993 standard on a JF-3 oxygen index tester (Nanjing Jiangning Analytical Instrument Factory, China) with sample dimensions of 150 mm × 10 mm × 10 mm.

3 Results and Discussion

3.1 Friedel-Crafts Reaction between TO and Phenol

To verify the success of the Friedel-Crafts reaction between TO and phenol, we recorded the FT-IR spectra of samples, collected at different times (0.5, 1, and 2 h) during the reaction, along –with the TO spectrum for comparison (Fig. 2). Before FT-IR acquisition, the samples were washed several times with hot water to remove free phenol. Characteristic TO absorption at 3104 cm^{-1} (=C–H stretching), 992 cm^{-1} (=C–H bending), and 1643 cm^{-1} (C=C stretching) are absent from all reaction products [26], indicateding that the conjugated triene bond in TO had undergone reaction. New absorption bands appeared at approximately 3388 cm^{-1} and 1227 cm^{-1}, which we attribute to stretching and bending vibrations, respectively, of the phenolic hydroxyl group. Bands at 1595 cm^{-1} and 1500 cm^{-1} represent benzene ring C=C skeletal vibrations [33]. These FTIR data indicate that the Friedel-Crafts reaction was successful in grafting phenol and TO. Furthermore, the products show new bands at 830 cm^{-1} and 752 cm^{-1}, which arise from the C–H bending modes of two neighboring hydrogen atoms on the bridging $–CH_2–$ groups and the four different benzene ring hydrogen atoms illustrating that the phenol ortho and para positions participate in the reaction. Based on these results, we conclude that the Friedel-Crafts reaction between the TO conjugated triene and phenol occurs at the ortho and para positions on phenol.

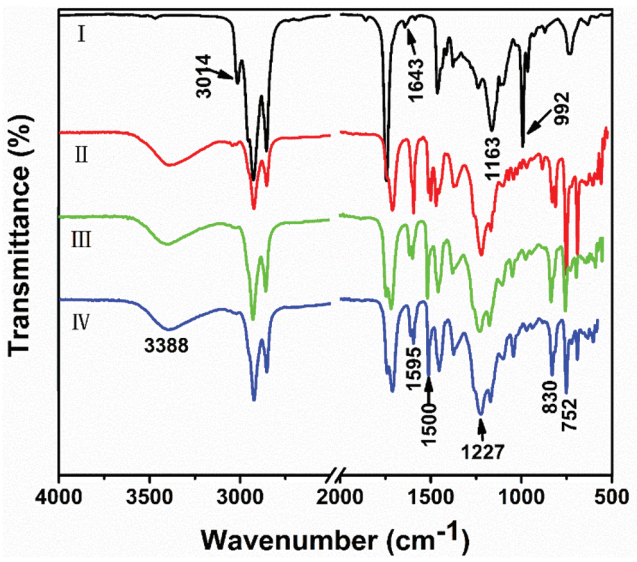

Figure 2: FT-IR spectra of TO and phenol Friedel-Crafts reaction at different times: (I) 0 h, (II) 0.5 h, (III) 1 h, (IV) 2 h

To further confirm the success of the Friedel-Crafts reaction, we acquired ^1H NMR spectra of the products after 1 h reaction time for compared with the TO ^1H NMR spectrum (Fig. 3). A new multiplet at around 6.75–7.25 ppm corresponds to protons in the benzene ring [33] (Fig. 3b). We attribute multiple peaks at around 5.36–6.38 ppm to conjugated bond protons of the TO moiety (–CH=CH–CH=CH–CH=CH–) [26].

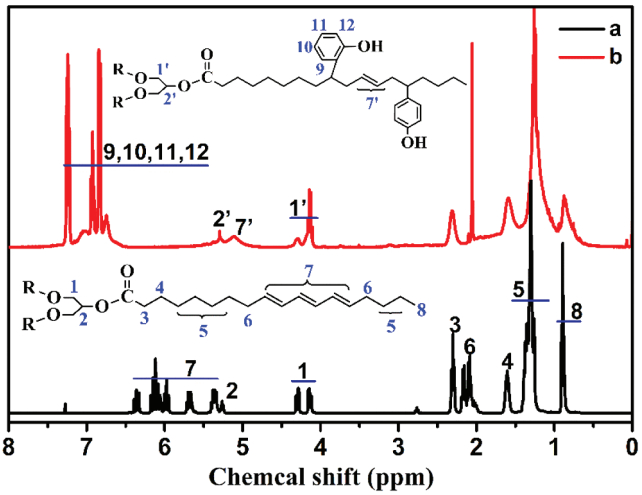

Figure 3: ^{1}H NMR spectra of TO (a) and sample (b) collected by reacting TO with phenol for 2 h

A broad single peak at 5.11 ppm belongs to protons of the –CH=CH– group [25]. Furthermore, the peak area integration is about 1/3 of the total integral for the triene-proton peak area in TO. Together with the FT-IR results, these data confirm that the two outer double bonds in the conjugated triene system participate in the reaction (Fig. 1). Thus, these results support the successful grafting of phenol onto the TO alkyl chain. The GPC and elemental analysis results of tung oil and pure tung oil-phenol reaction products are shown in Tab. 1. Elemental analysis has 5% measurement error. Comparing the calculated values with the actual calculated values in Tab. 1 illustrates that 1 mole of tung oil has reacted with approximately 6 moles of phenol. The relative molecular weight of tung oil measured by GPC method is 1460 (theoretical calculated value (Calc.): 873), according to this, the relative molecular weight of tung oil-phenol should be 1460 + 6 × 94 = 2025 (Calc.: 1438). The actual measured results for Tung oil-phenol are 1851 g/mol (TPF3) and 2377 g/mol (TPF12), respectively, which basically accord with the theoretical values.

Table 1: Relative molecular mass and elementary analysis of tung oil and pure tung oil-phenol reaction products

	[a]Mw (g/mol)		C content (%)		H content (%)		O content (%)	
Samples	[b]Calc.	[c]Act.	Calc.	Act.	Calc.	Act.	Calc.	Act.
[d]Tung oil	873	1460	78.44	77.79	10.55	10.65	11.01	11.56
[e]Tung oil-phenol (TPF3)	1438	1851	77.61	73.62	8.90	8.59	13.49	17.79
Tung oil-phenol (TPF12)	1438	2377	77.61	74.48	8.90	9.12	13.49	16.40

a: Weight-average molar mass; b: Calculated value; c: Actual value; d: The Calc. of tung oil is calculated based on the main component of eleostearic acid ester in tung oil; e: The Calc. of tung oil-phenol is calculated by reacting 1 mole of tung oil with 6 moles of phenol.

3.2 Mechanical Properties

We determined the mechanical properties of pure PF and of TPF samples by performing static compression and bending tests. Tab. 2 lists the apparent density, compressive strength, and flexural strengths. Both compressive and flexural strengths show increases over pure PF for TPF 3, TPF 6, and TPF 9 (Fig. 4a). TPF-6 exhibits greatest compressive and flexural strengths of 0.278 ± 0.036 MPa and

Table 2: Mechanical properties and resin's free formaldehyde of pure PF and TPFs

Samples	Density (Kg/m3)	Compressive strength (MPa)	Flexural strength (MPa)	Free formaldehyde (%)
Pure PF	53.72 ± 1.49	0.160 ± 0.045	0.241 ± 0.060	0.17
TPF-3	52.99 ± 1.22	0.206 ± 0.014	0.320 ± 0.010	0.22
TPF-6	53.90 ± 1.14	0.278 ± 0.036	0.450 ± 0.017	0.37
TPF-9	51.54 ± 2.11	0.225 ± 0.012	0.360 ± 0.011	0.59
TPF-12	56.78 ± 0.75	0.155 ± 0.010	0.234 ± 0.017	1.01

0.450 ± 0.017 MPa, respectively, representing increases of 68.75% and 86.72% over pure PF. This improvements are the result of introducing the phenolic long alkyl chains into the foam's molecular structure. The long alkyl chains provide increased flexibility and enhanced toughness in the TPFs [7,34]. However, the compressive and flexural strengths of TPF-12 are similar to those of pure PF and show little change. The absence of any improvement for TPF-12 is because the introduction of large amounts of TO reduces the reactivity of the resin, resulting in imperfect curing. Fig. 4b shows that the resin's free formaldehyde of pure PF and TPFs gradually increases with the TO content increasing. This mainly from the presence of alkyl side chains increases steric hindrance, thereby hindering the reaction of formaldehyde with phenol and reducing the reactivity of synthetic resins.

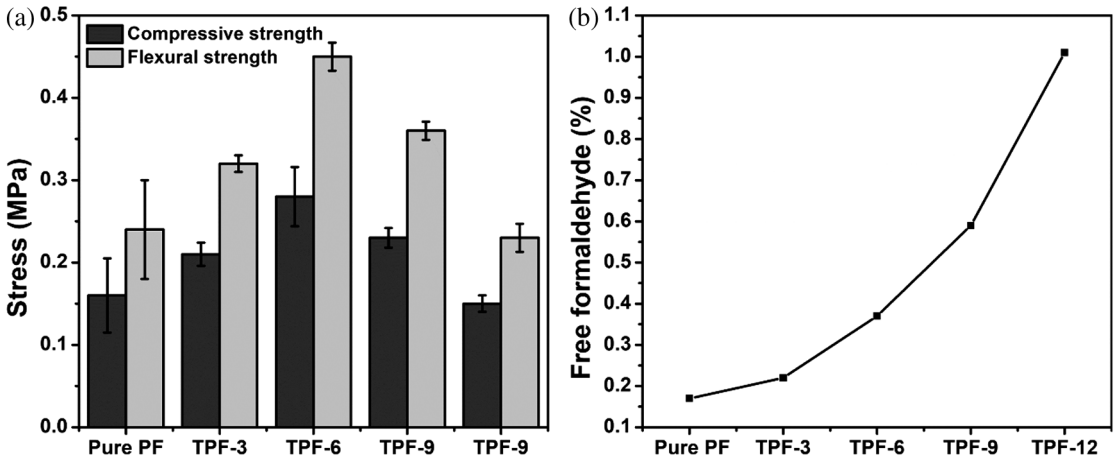

Figure 4: Mechanical properties and resin's free formaldehyde of pure PF and TPFs

To further investigate the effects of TO on the mechanical properties of foams, we observed the microstructure of pure PF and TPFs using scanning electron microscopy (SEM). Fig. 5 shows the foam structures comprising closed cells. The addition of TO significantly decreases the cell size of the phenolic foams. Pure PF has a mean pore diameter of 168.50 μm. The mean pore diameters of TPF-3, TPF-6, TPF-9, and TPF-12 are 154.18 μm, 96.53 μm, 120.77 μm, and 153.40 μm, respectively, which represent decreases of 8.50%, 42.71%, 28.33%, and 8.96% compared with those of pure PF. Moreover, the size of the cells for TPFs are more uniform than they are in pure PF, which ranges from 120 to 240 μm. TPF-6, by contrast, exhibits a very narrow pore size distribution (from 70 to 140 μm). Remarkably, the TPF cells are hexagonal (Fig. $5e_1$) and form a stable honeycomb-like structure, which contrasts with the ellipsoid-like cells exhibited by pure PF. In summary, TPF 6 features a smaller pore size, a narrower pore size

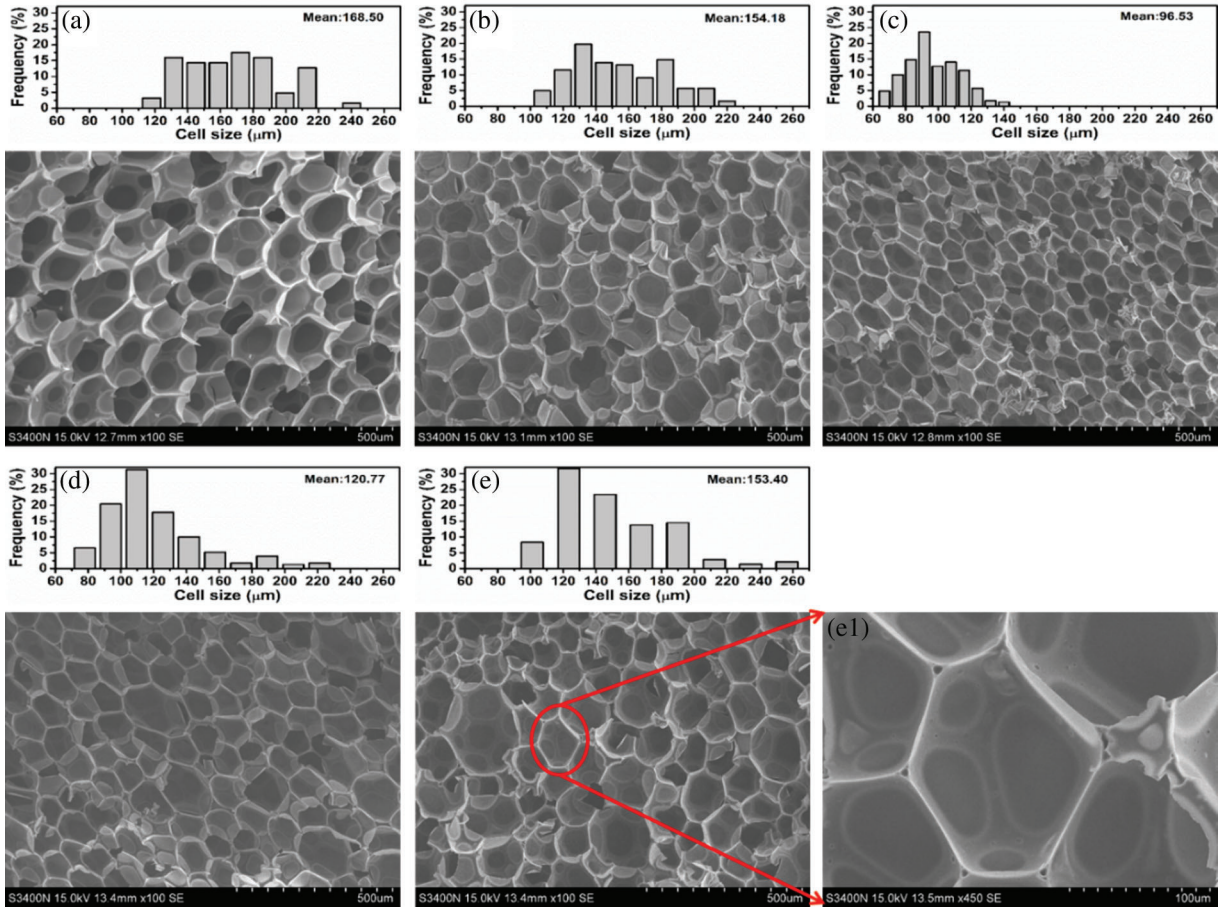

Figure 5: SEM and cell sizes distribution of Pure PF and TPFs: (a) Pure PF; (b) TPF-3; (c) TPF-6; (d) TPF-9; (e, e_1) TPF-12

distribution, and a hexagonal cell geometry that provides the most robust mechanical properties among all samples [35].

3.3 Thermal Stability of Pure PF and TPFs

Thermal stability refers to the ability of a material to withstand rapid changes in temperature without damage, also known as thermal shock resistance. We assessed the thermal stabilities of pure PF and TPFs derivatives using thermogravimetric analysis (TGA). Fig. 6 shows the TGA and derivative thermogravimetric (DTG) curves, and Tab. 3 summarizes relevant degradation data. Pure PF has three main decomposition temperatures. Mass loss arise mainly from foaming agent volatilization and loss of water, free phenol, and Tween 80 (Step I: 40–200°C), diphenyl ether bond condensation-dehydration (Step II: 200–400°C), and degradation of the methylene-bridged structure and long-chain (Step III: 400–800°C), respectively [36]. Tab. 3 shows that the temperature at 5% mass loss ($T_{-5\%}$) for the TPF samples is slightly higher than that for pure PF (106.3°C). DTG curves show that TPF samples have lower degradation rates than pure PF throughout the pyrolysis process. However, the maximum decomposition temperatures for step I and step III, and the TPF residual masses are significantly lower than those for pure PF. The flexible alkyl long chain introduced into the phenolic foam matrix facilitates the thermal motion of resin chains and facilitates the rapid removal of volatile decomposition product flux to exit

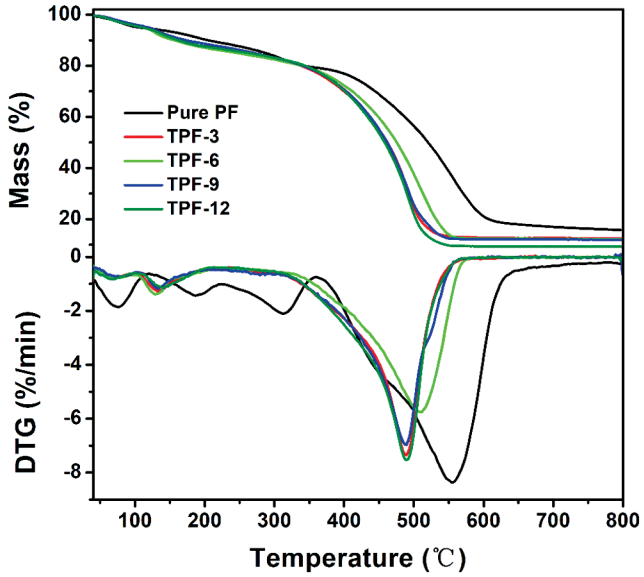

Figure 6: TGA and DTG curves of pure PF and TPFs in O_2 atmosphere

Table 3: TGA date of pure PF and TPFs in O_2 atmosphere.

Samples	Density (Kg/m^3)	$T_{-5\%}$ (°C)	T_{max} (°C)			Residual mass (%)
			Step I	Step II	Step III	
Pure PF	53.72 ± 1.49	106.3	186.7	312.4	556.4	15.7
TPF-3	52.99 ± 1.22	114.2	131.7	/	488.4	12.5
TPF-6	53.90 ± 1.14	111.7	129.2	/	508.0	12.2
TPF-9	51.54 ± 2.11	119.1	131.6	/	488.7	12.0
TPF-12	56.78 ± 0.75	111.5	141.5	/	489.9	9.2

from cell walls. Moreover, the thermal stability of the alkyl chains is much less than that for the rigid benzene rings. These factors suggest that TO modification impairs the heat resistance of phenolic foams [6].

3.4 Flame-Retardant Properties of Pure PF and TPFs

The commonly used limiting oxygen index (LOI) is a useful parameter for evaluating the combustion performance of materials. The LOI refers to the minimum oxygen concentration required for materials to maintain combustion in a mixed gas stream of oxygen and nitrogen. We generally express stream composition as a percentage of oxygen of the total volume. Pure PF, a flame-retardant material, has an LOI of 38.9%. Fig. 7 shows the LOIs data of pure PF and TPFs. The figure reveals significantly decreasing LOI values for foams with increasing TO content. TPF-3 and TPF-6, with LOI values of 34.6%, and 27.5%, respectively, each exceed the 27% boundary considered necessary for flame retardant materials. LOI values for TPF-9 and TPF-12 are 25.2%, and 23.8%, respectively, characterizing these foams as combustible. The addition of TO has a significant impact on the foam LOI values. TGA testing reveals that carbonization rates of TO modified phenolic foams are low because the long alkyl is less stable upon heating than the benzene ring. Pure PF burns to form a black and solid blocky charred residue. The TPF combustion residue layer becomes thinner, softer, and more powdery with increasing

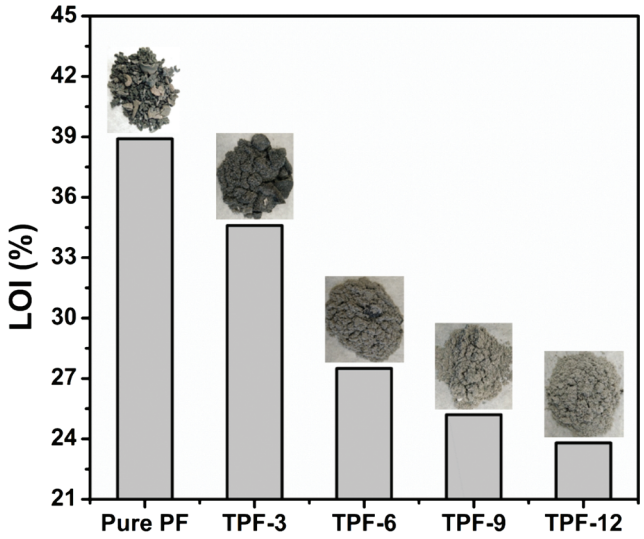

Figure 7: LOIs, and char residue photographs of pure PF and TPFs

TO content. Additionally, the residue becomes a lighter shade of grey. Thin and soft char residue layers are not effective barriers to heat and oxygen transfer in the foam solid [37]. Therefore, the TPF samples' LOI values decrease with increasing TO content.

Cone calorimetry is a practical test method for simulating real fire conditions. We characterized the combustion-heat release and smoke-release behaviors of pure PF and TPF-12 by cone calorimetry (Fig. 8 and Tab. 4). Time to ignition (TTI) is the time taken for the surface of a material to ignite, which is a parameter for evaluating the fire resistance of a material. The heat release rate (HRR), and the peak heat release rate (pHRR) in particular, are essential parameters for assessing the flame-retardant properties of materials by cone calorimetry. The smaller the HRR and pHRR values, the better the flame retardancy of the material, and vice versa. The test results reveal that the introduction of long alkyl chains considerably increases the HRR and shortens the TTI of phenolic foams. The pHRR and TTI for pure PF are 38.19 kW/m^2 and 56 s, respectively, while the pHRR for TPF-12 rises to 46.30 kW/m^2 and the TTI shortens to 15 s. The change in mean heat release rate (mHRR) shows a similar trend, from 15.87 kW/m^2 for pure PF up to 16.15 kW/m^2 for TPF-12. As shown by the total heat release curve (THR) (Fig. 8b), TPF-12 has a slightly larger THR value compared with that for pure PF. After burning for 1200 s, the TPF-12 and pure PF THR values are 19.20 MJ/m^2 and 18.45 MJ/m^2, respectively. Additionally, the residual mass for TPF-12 after combustion (0.84%) is significantly less than that for pure PF (7.81%) (Tab. 4). This observation suggests that the presence of long alkyl chains reduces the foam's ability to form a protective carbon layer and insulate from heat effectively, cut off oxygen, and inhibit the combustion of the foam, thereby reducing the HRR and THR during combustion [38,39].

The smoke released by the burning materials in a fire is hazardous and toxic. It can poison personnel or cause asphyxiation, both are significant causes of death, so smoke suppression by flame-retardant materials is particularly important. The cone calorimetry test can provide information about smoke release during combustion, including the smoke release rate (RSR) and total smoke release (TSR) (Fig. 8c,d). Although the peak smoke release rate (pRSR) for TPF-12 (0.39 $m^2/m^2/s$) is greater than that for pure PF (0.15 $m^2/m^2/s$), the RSR for TPF-12 is consistently lower than that for pure PF. The TSR for pure PF is 30.15 m^2/m^2. The TSR shows increases over pure PF for TPFs (Fig. 8d). The value for TSR is linearly related to the proportion of tung oil content in the foams. The r^2 value is 0.985, revealing that the fitted results are in great agreement with the measured results. TPF-12 exhibits least TSR of 7.77 m^2/m^2, representing reduction of 74.23% over

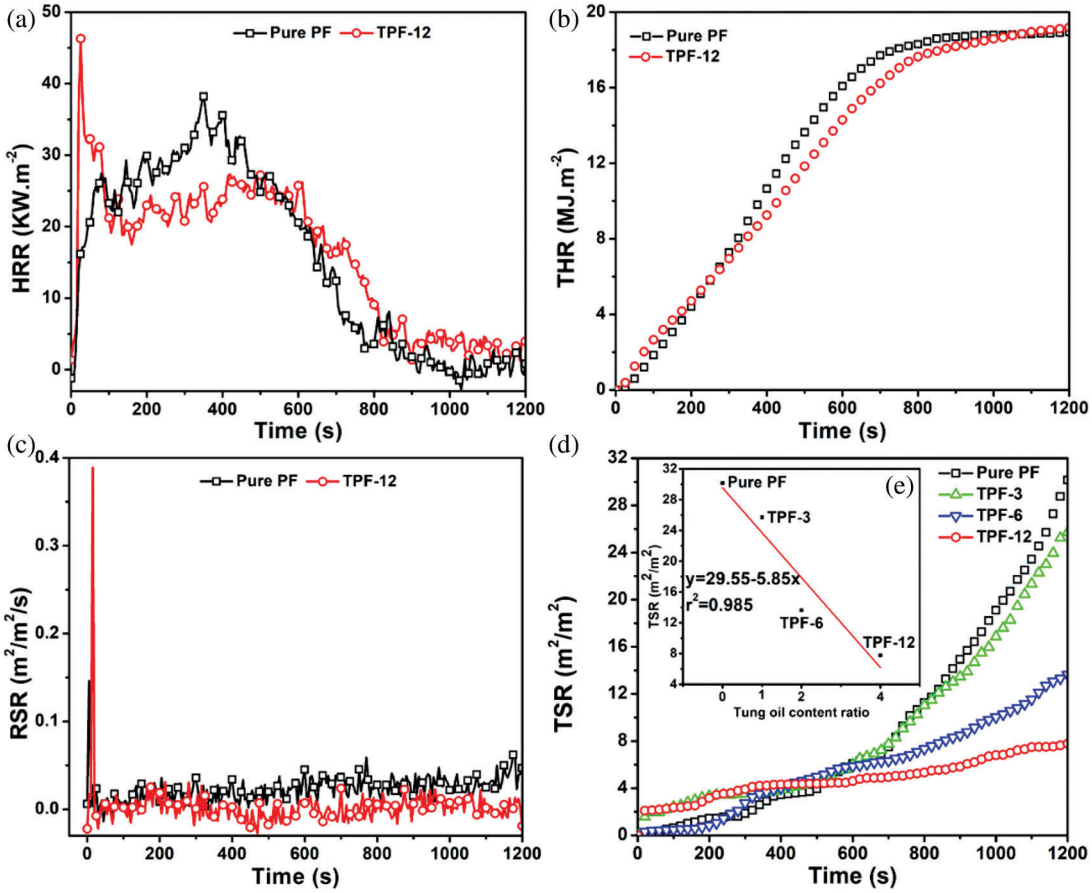

Figure 8: Cone calorimetric test results of pure PF and TPF-12: (a) heat release rate (HRR); (b) total heat release (THR); (c) release smoke rate (RSR); (d) total smoke release (TSR) of TPF-3, TPF-6 and TPF-12; (e) the TSR (y) variation as a function of tung oil content ratio (x)

Table 4: Cone calorimetric test data

Samples	TTI[a] (s)	HRR (kW/m^2)		THR (MJ/m^2)	pSRS (m^2/m^2/s)	TSR (m^2/m^2)	Residual mass (%)
		pHRR[b]	mHRR[c]				
Pure PF	56	38.19	15.87	18.45	0.15	30.15	7.81
TPF-12	15	46.30	16.15	19.20	0.39	7.77	0.84

a: TTI – time to ignition; b: HRR – the peak value of HRR; c: HRR – the mean of HRR.

pure PF. The smaller the TSR value, the smaller the amount of smoke released by the material in a fire. These data indicate that smoke inhibition by TO modified phenolic foams provides a significant improvement over pure PF, while at the same time, the material can fully and effectively burn, which we mainly attribute to the ability of the long alkyl chains in the TO substituent to reduce char formation.

4 Conclusions

We fabricated novel tung-oil-toughened phenolic foams (TPFs) with enhanced mechanical and smoke suppression properties. SEM micrographs reveal that the TPFs microstructures offer advantages over pure

PF, including more uniform hexagon-cell morphology, narrower cell size distribution ranges, and smaller mean cell sizes, which are beneficial to the observed improvements in mechanical properties. Specifically, compared with pure PF, the mechanical properties of TPF-6 increased by 68.75% in compressive strength and by 86.72% in flexural strength. TPF 6 has an LOI value of 27.5%, which classifies this material as a refractory material. Total smoke release for TPF-12 is 74.23% less than that of pure PF, indicating that the long alkyl chains in tung oil significantly improve smoke suppression of the combusting foam. However, due to flammability of the long alkyl chains, the TPF modified foams suffer reduced thermal stability and high-temperature charring rates, higher peak and mean heat release rates, and greater total heat release than pure PF. Therefore, future research should investigate the modification of tung oil to improve its flame-retardant properties and those of the toughened foams.

Acknowledgement: The authors are grateful to the financial support from the Fundamental Research Funds for the Central Non-profit Research Institution of CAF (No. CAFYBB2018MA001) and the National Natural Science Foundation of China (Grant No. 31700499).

Funding Statement: The author(s) received no specific funding for this study.

Conflicts of Interest: The authors declare that they have no conflicts of interest to report regarding the present study.

References

1. Bo, C., Yang, X., Hu, L., Zhang, M., Jia, P. et al. (2018). Enhancement of flame-retardant and mechanical performance of phenolic foam with the incorporation of cardanol-based siloxane. *Polymer Composites, 40(6),* 2539–2547. DOI 10.1002/pc.25285.
2. Zhang, N., Hu, L., Guo, Y., Bo, C., Jia, P. et al. (2020). Mechanical property of lignin-modified phenolic foam enhanced by whisker silicon. *Journal of Dispersion Science and Technology, 41(3),* 348–354. DOI 10.1080/01932691.2019.1578662.
3. Si, J., Tawiah, B., Sun, W., Lin, B., Wang, C. et al. (2019). Functionalization of MXene nanosheets for polystyrene towards high thermal stability and flame retardant properties. *Polymers, 6(11),* 976. DOI 10.3390/polym11060976.
4. Shi, Y., Liu, C., Fu, L., Yang, F., Lv, Y. et al. (2019). Hierarchical assembly of polystyrene/graphitic carbon nitride/reduced graphene oxide nanocomposites toward high fire safety. *Composites Part B: Engineering, 179,* 107541. DOI 10.1016/j.compositesb.2019.107541.
5. Zhou, W., Bo, C., Jia, P., Zhou, Y., Zhang, M. (2019). Effects of tung oil-based polyols on the thermal stability, flame retardancy, and mechanical properties of rigid polyurethane foam. *Polymers, 11(1),* 45. DOI 10.3390/polym11010045.
6. Liang, B., Li, X., Hu, L., Bo, C., Zhou, J. et al. (2016). Foaming resol resin modified with polyhydroxylated cardanol and its application to phenolic foams. *Industrial Crops and Products, 80,* 194–196. DOI 10.1016/j.indcrop.2015.11.087.
7. Bo, C., Wei, S., Hu, L., Jia, P., Liang, B. et al. (2016). Synthesis of a cardanol-based phosphorus-containing polyurethane prepolymer and its application in phenolic foams. *RSC Advances, 6(67),* 62999–63005. DOI 10.1039/C6RA08249A.
8. Guo, Y., Hu, L., Jia, P., Zhang, B., Zhou, Y. (2018). Enhancement of thermal stability and chemical reactivity of phenolic resin ameliorated by nanoSiO_2. *Korean Journal of Chemical Engineering, 35(1),* 298–302. DOI 10.1007/s11814-017-0240-9.
9. Wei, D., Li, D., Zhang, L., Zhao, Z., Ao, Y. (2012). Study on phenolic resin foam modified by montmorillonite and carbon fibers. *Procedia Engineering, 27,* 374–383. DOI 10.1016/j.proeng.2011.12.465.
10. Gao, M., Wu, W., Wang, Y., Wang, Y., Wang, H. (2016). Phenolic foam modified with dicyandiamide as toughening agent. *Journal of Thermal Analysis and Calorimetry, 124(1),* 189–195. DOI 10.1007/s10973-015-5156-1.

11. Liu, L., Fu, M., Wang, Z. (2015). Synthesis of boron-containing toughening agents and their application in phenolic foams. *Industrial & Engineering Chemistry Research, 54(7),* 1962–1970. DOI 10.1021/ie504851y.
12. Yu, Z., Li, J., Yang, L., Yao, Y., Su, Z. et al. (2012). Synthesis and properties of nano carboxylic acrylonitrile butadiene rubber latex toughened phenolic resin. *Journal of Applied Polymer Science, 123(2),* 1079–1084. DOI 10.1002/app.34573.
13. Song, F., Jia, P., Xiao, Y., Bo, C., Hu, L. et al. (2019). Study on toughening phenolic foams in phosphorus-containing tung oil-based derivatives. *Journal of Renewable Materials, 7(10),* 1011–1021. DOI 10.32604/jrm.2019.08044.
14. Hu, L., Zhou, Y., Liu, R., Zhang, M., Yang, X. (2013). Synthesis of foaming resol resin modified with oxidatively degraded lignosulfonate. *Industrial Crops and Products, 44,* 364–366. DOI 10.1016/j.indcrop.2012.11.034.
15. Hu, L., Zhou, Y., Liu, R., Zhang, M. (2012). Phenolic foam from oxidatively degradated lignosulphonate. *Advanced Materials Research, 581,* 238–241. DOI 10.4028/www.scientific.net/AMR.581-582.238.
16. Bo, C., Hu, L., Chen, Y., Yang, X., Zhang, M. et al. (2018). Synthesis of a novel cardanol-based compound and environmentally sustainable production of phenolic foam. *Journal of Materials Science, 53(15),* 10784–10797. DOI 10.1007/s10853-018-2362-9.
17. Jia, P., Song, F., Li, Q., Xia, H., Li, M. et al. (2019). Recent development of cardanol based polymer materials-a review. *Journal of Renewable Materials, 7(7),* 601–619. DOI 10.32604/jrm.2019.07011.
18. Li, J., Zhang, A., Zhang, S., Gao, Q., Zhang, W. et al. (2019). Larch tannin-based rigid phenolic foam with high compressive strength, low friability, and low thermal conductivity reinforced by cork powder. *Composites Part B: Engineering, 156,* 368–377. DOI 10.1016/j.compositesb.2018.09.005.
19. Ma, Y., Gong, X., Xie, B., Geng, X., Jia, P. (2019). Synthesis and characterization of DOPO-g-CNSL and its effect on the properties of phenolic foams. *Journal of Renewable Materials, 7(10),* 1037–1046. DOI 10.32604/jrm.2019.07454.
20. Jia, P., Ma, Y., Xia, H., Zheng, M., Feng, G. et al. (2018). Clean synthesis of epoxidized tung oil derivatives via phase transfer catalyst and thiol-ene reaction: a detailed study. *ACS Sustainable Chemistry & Engineering, 6(11),* 13983–13994. DOI 10.1021/acssuschemeng.8b02446.
21. Huang, K., Liu, Z., Zhang, J., Li, S., Li, M. et al. (2014). Epoxy monomers derived from tung oil fatty acids and its regulable thermosets cured in two synergistic ways. *Biomacromolecules, 15(3),* 837–843. DOI 10.1021/bm4018929.
22. Sharma, V., Das, L., Pradhan, R. C., Naik, S. N., Bhatnagar, N. et al. (2011). Physical properties of tung seed: an industrial oil yielding crop. *Industrial Crops and Products, 33(2),* 440–444. DOI 10.1016/j.indcrop.2010.10.031.
23. Liang, B., Zhao, J., Li, G., Huang, Y., Yang, Z. et al. (2019). Facile synthesis and characterization of novel multi-functional bio-based acrylate prepolymers derived from tung oil and its application in UV-curable coatings. *Industrial Crops & Products, 138,* 111585. DOI 10.1016/j.indcrop.2019.111585.
24. Xu, X., Chen, L., Guo, J., Cao, X., Wang, S. (2017). Synthesis and characteristics of tung oil-based acrylated-alkyd resin modified by isobornyl acrylate. *RSC Advances, 7(48),* 30439–30445. DOI 10.1039/C7RA02189E.
25. Liu, C., Wu, Q., An, R., Shang, Q., Feng, G. et al. (2019). Synthesis and properties of tung oil-based unsaturated co-ester resins bearing steric hindrance. *Polymers, 11(5),* 826. DOI 10.3390/polym11050826.
26. Huang, J., Yuan, T., Ye, X., Man, L., Zhou, C. et al. (2018). Study on the UV curing behavior of tung oil: mechanism, curing activity and film-forming property. *Industrial Crops & Products, 112,* 61–69. DOI 10.1016/j.indcrop.2017.10.061.
27. Jia, P., Hu, L., Yang, X., Zhang, M., Shang, Q. et al. (2017). Internally plasticized PVC materials via covalent attachment of aminated tung oil methyl ester. *RSC Advances, 7(48),* 30101–30108. DOI 10.1039/C7RA04386D.
28. Xiao, L., Liu, Z., Hu, F., Wang, Y., Huang, J. et al. (2019). A renewable tung oil-derived nitrile rubber and its potential use in epoxy-toughening modifiers. *RSC Advances, 9(44),* 25880–25889. DOI 10.1039/C9RA01918A.
29. Yoshimura, Y., Nomoto, M. (1986). Products characterization of tung oil-phenol reactions based on analysis of a model reaction. *Journal of Polymer Science Part A: Polymer Chemistry, 24(9),* 2351–2372. DOI 10.1002/pola.1986.080240926.

30. Gang, Y., Pengsun, L., Yu, W., Hong, Y. (1994). Study on phenol-formaldehyde resins modified with tung oil (I)–synthesis, mechanism and characterization. *Chemistry and Industry of Forest Products, 14(4),* 23–31.
31. Meixiu, S., Min, C., Xinhua, Y., Xiaonong, C. (2005). Study on phenolic resin modified with tung oil and its application to brake block. *Engineering Plastics Application, 33(7),* 33–35.
32. Li, Y., Zhou, Y. K., Yao, J. (2010). Research on friction performance of the brake band based on the phenolic resin binary modified with boric acid & tung oil. *Lubrication Engineering, 35(4),* 43–46.
33. Yoshimura, Y. (1983). Reaction of 3-methyl phenol with tung oil. *Journal of Applied Polymer Science, 28(3),* 1147–1158. DOI 10.1002/app.1983.070280320.
34. Yang, Y., He, J. (2015). Mechanical characterization of phenolic foams modified by short glass fibers and polyurethane prepolymer. *Polymer Composites, 9(36),* 1584–1589. DOI 10.1002/pc.23066.
35. Luo, X., Yu, K., Qian, K. (2018). Morphologies and compression performance of graphene oxide/SiO_2 modified phenolic foam. *High Performance Polymers, 30(7),* 803–811. DOI 10.1177/0954008317731136.
36. Yuan, J., Zhang, Y., Wang, Z. (2015). Phenolic foams toughened with crosslinked poly(n-butyl acrylate)/silica core-shell nanocomposite particles. *Journal of Applied Polymer Science, 132(40),* 42590. DOI 10.1002/app.41218.
37. Li, Q., Chen, L., Li, X., Zhang, J., Zhang, X. et al. (2016). Effect of multi-walled carbon nanotubes on mechanical, thermal and electrical properties of phenolic foam via in-situ polymerization. *Composites Part A: Applied Science and Manufacturing, 82,* 214–225. DOI 10.1016/j.compositesa.2015.11.014.
38. Jia, P., Zhang, M., Hu, L., Zhou, J., Feng, G. et al. (2015). Thermal degradation behavior and flame retardant mechanism of poly(vinyl chloride) plasticized with a soybean-oil-based plasticizer containing phosphaphenanthrene groups. *Polymer Degradation and Stability, 121,* 292–302. DOI 10.1016/j.polymdegradstab.2015.09.020.
39. Jia, P., Hu, L., Zhang, M., Feng, G., Zhou, Y. (2017). Phosphorus containing castor oil based derivatives: potential non-migratory flame retardant plasticizer. *European Polymer Journal, 87,* 209–220. DOI 10.1016/j.eurpolymj.2016.12.023.